

# Targeted Suppression of Peptide Degradation in Ag-Based Surface-Enhanced Raman Spectra by Depletion of Hot Carriers

Xiaobin Yao, Christiane Höppener, Henrik Schneidewind, Stephanie Hoepfener, Zian Tang, Axel Buchholz, Annika König, Selene Mogavero, Marco Diegel, Jan Dellith, Andrey Turchanin, Winfried Plass, Bernhard Hube, and Volker Deckert\*

Sample degradation, in particular of biomolecules, frequently occurs in surface-enhanced Raman spectroscopy (SERS) utilizing supported silver SERS substrates. Currently, thermal and/or photocatalytic effects are considered to cause sample degradation. This paper establishes the efficient inhibition of sample degradation using iodide which is demonstrated by a systematic SERS study of a small peptide in aqueous solution. Remarkably, a distinct charge separation-induced surface potential difference is observed for SERS substrates under laser irradiation using Kelvin probe force microscopy. This directly unveils the photocatalytic effect of Ag-SERS substrates. Based on the presented results, it is proposed that plasmonic photocatalysis dominates sample degradation in SERS experiments and the suppression of typical SERS sample degradation by iodide is discussed by means of the energy levels of the substrate under mild irradiation conditions. This approach paves the way toward more reliable and reproducible SERS studies of biomolecules under physiological conditions.

## 1. Introduction

Raman spectroscopy allows for analyzing materials based on their intrinsic vibrational information.<sup>[1]</sup> However, low Raman


cross-sections of molecules limit the detection of trace amounts of samples. The advent of surface-enhanced Raman spectroscopy (SERS) well overcomes this drawback.<sup>[2]</sup> Benefiting from surface plasmon resonance effects and/or chemical effects, Raman signals can be enhanced up to 10 to 12 orders of magnitude in SERS.<sup>[3]</sup> Currently, SERS is widely applied in the fields of chemical and structural analysis, drug detection, forensic science, etc.<sup>[2,4]</sup> However, frequently observed sample degradation in SERS experiments,<sup>[5–7]</sup> especially when silver nanoparticle-based SERS is applied, requires an in-depth investigation of the underlying principles. This issue accounts particularly for fragile materials, such as biological samples.<sup>[8,9]</sup>

Various plasmonic materials (material, shape, preparation methods) have been applied in SERS studies. Most often colloids made by chemical reduction methods or substrates prepared by physical vapor deposition (PVD) are used.<sup>[2]</sup> An essential difference between both approaches is the degree of potential chemical contamination induced during the

X. Yao, C. Höppener, H. Schneidewind, M. Diegel, J. Dellith, V. Deckert  
Leibniz Institute of Photonic Technology (IPHT)  
Albert-Einstein-Str. 9, 07745 Jena, Germany  
E-mail: volker.deckert@uni-jena.de

X. Yao, C. Höppener, Z. Tang, A. Turchanin, V. Deckert  
Institute of Physical Chemistry (IPC) and Abbe Center of Photonics  
Friedrich Schiller University Jena  
Lessingstr. 10, 07743 Jena, Germany

S. Hoepfener  
Jena Center for Soft Matter (JCSM)  
Friedrich Schiller University Jena  
Philosophenweg 7, 07743 Jena, Germany

 The ORCID identification number(s) for the author(s) of this article can be found under <https://doi.org/10.1002/sml.202205080>.

© 2022 The Authors. Small published by Wiley-VCH GmbH. This is an open access article under the terms of the Creative Commons Attribution-NonCommercial-NoDerivs License, which permits use and distribution in any medium, provided the original work is properly cited, the use is non-commercial and no modifications or adaptations are made.

DOI: 10.1002/sml.202205080

S. Hoepfener  
Laboratory of Organic and Macromolecular Chemistry  
Friedrich Schiller University Jena  
Humboldtstr. 10, 07743 Jena, Germany

A. Buchholz, W. Plass  
Institute of Inorganic and Analytical Chemistry (IAAC)  
Friedrich Schiller University Jena  
Humboldtstr. 8, 07743 Jena, Germany

A. König, S. Mogavero, B. Hube  
Department of Microbial Pathogenicity Mechanisms  
Leibniz Institute for Natural Product Research and Infection  
Biology – Hans Knöll Institute (HKI)  
Beutenbergstrasse 11a, 07745 Jena, Germany

B. Hube  
Institute of Microbiology  
Friedrich Schiller University Jena  
Neugasse 25, 07743 Jena, Germany

V. Deckert  
Institute For Quantum Science and Engineering (IQSE)  
Texas A&M University  
College Station, TX 77843, USA

preparation process, intrinsically avoided when using PVD. Aside from the possible contaminations, sample degradation particularly of bio-samples on such PVD-fabricated SERS substrates is another severe issue. A hallmark of sample degradation in SERS investigations is the appearance of one or two large and broad bands located around 1350 and 1570  $\text{cm}^{-1}$  respectively, which can be assigned to carbonaceous fragments of the sample.<sup>[10]</sup> Once sample degradation occurs, parts of the observed Raman signals derive from the formed fragments rather than from the original sample, rendering an assignment even under the best conditions challenging. Consequently, it is almost impossible to compare the SERS spectra to reference Raman spectra, as these bands obscure a reliable assignment of Raman bands of the exact sample.

While the enhancement capabilities of SERS substrates are largely associated with the radiative decay of the excited localized surface plasmon resonances, multiple studies rationalized that competing non-radiative decay routes can lead to photothermal and plasmonic photocatalytic effects.<sup>[11,12]</sup> To date, both effects have also been recognized as potential causes for an undesired sample degradation in SERS, which may induce the observed spectral and eventually structural changes. Some groups consider that the photothermal effect dominates the sample degradation.<sup>[13,14]</sup> Local heating obviously can break chemical bonds, in particular for most biological samples the temperatures required for a (short-term) decomposition of matter are considerably high in comparison to temperatures reached in plasmon-enhanced approaches.<sup>[15]</sup> Experiments that directly detect the temperature by considering the Stokes to Anti-Stokes ratio in combination with the specific plasmon resonance of single particles yield elevated ( $\approx 70$  °C), but not extremely high temperatures leading to temperature-induced burning.<sup>[16]</sup> Such photothermal degradation must not be confused with denaturing of, e.g., proteins, which will lead to secondary structure changes, but not to a decomposition. In contrast to the thermal effect, it has been reported that Ag nanoparticles can act as a plasmonic photocatalyst due to the plasmon decay, which can cause various redox reactions.<sup>[17–19]</sup> In photocatalysis hot electrons ( $e^-$ ) and holes ( $h^+$ ) are formed on the surface of the photocatalyst that either will quickly recombine and/or interact with the sample in the vicinity of these particles. For example, it has been reported that the plasmon-supported reaction of  $\text{H}_2\text{O}$  leads to the formation of radicals like hydroxyl radicals ( $\cdot\text{OH}$ ) and superoxide radicals ( $\cdot\text{O}_2^-$ ).<sup>[20]</sup> Both radicals can assuredly induce efficient sample degradations. Notably, the energy of generated hot carriers will be determined by the Fermi level of Ag nanoparticles and the input photons.<sup>[19,21]</sup> Moreover, it has to be considered that the unavoidable oxidation of Ag under ambient conditions leads to property changes in such Ag-nanoparticle (AgNP) systems.<sup>[22,23]</sup> As such, due to the oxidation of Ag,  $\text{Ag}_2\text{O}$  will partially cover the surface of plasmonic AgNPs and further affect the photocatalytic process. The naturally formed  $\text{Ag}_2\text{O}$  is a photocatalyst itself with a narrow band gap of 1.2 eV.<sup>[24,25]</sup> As a result, commonly used lasers for Raman spectroscopy (or SERS) at 532, 633, and even 785 nm can excite  $\text{Ag}_2\text{O}$ . The formed thin  $\text{Ag}_2\text{O}$  film essentially acts as a plasmon-assisted photocatalyst  $\text{Ag}_2\text{O}@$ Ag system which has a relatively stable structure and can support an efficient spatial charge separation.<sup>[18,26,27]</sup> Thus, active hot

carriers with an efficient lifetime can potentially cause chemical reactions and sample degradation in Ag-SERS experiments. Nevertheless, there is currently no common opinion on the respective influence of these effects.

The detailed mechanism behind sample degradation in SERS experiments is still under discussion. In this work, we present a new explanation for the possible degradation mechanism present in Ag SERS configurations. Photocatalysis is proposed to be the dominant effect, which is supported by the occurrence of a charge separation on the irradiated Ag-SERS substrate detected by Kelvin probe force microscopy (KPFM). Meanwhile, it was found that iodide can effectively suppress sample degradation of a peptide on a PVD-fabricated Ag-SERS substrate, as is supposed to react with the main hot carriers and then protect the samples.

## 2. Results and Discussion

### 2.1. Investigation of Peptide Degradation on Ag-Based SERS Substrates

The influence of the thermal effect causing sample degradation has been well investigated in Raman spectroscopy. There, the degradation could be minimized by using a low laser power,<sup>[28,29]</sup> however, usually at the cost of decreasing the signal-to-noise ratio. It is also suggested to use a suitable medium, like water, to dissipate the heat more efficiently.<sup>[30]</sup> Unfortunately, these strategies do not always work, as exemplified in **Figure 1**, which shows SERS spectra of a small peptide deuterated Candidalysin (dCaL) under different excitation powers in liquid measurements. 10  $\mu\text{L}$  of a 140  $\mu\text{mol L}^{-1}$  dCaL solution was dropped onto a clean glass slide. Each spectrum was averaged from 300 accumulations with 1 s acquisition time. With the increase of laser power, sample degradation becomes more pronounced. The two broad peaks at 1350 and 1570  $\text{cm}^{-1}$  indicate sample burning (labeled by green columns). The bands at low laser powers are assumed to originate from fragments of the peptide degraded by hot carriers. Sample degradation already begins at a power as low as 0.8  $\mu\text{W}$ . It is therefore unlikely that thermal effects play a major role, more likely other effects like plasmonic photocatalysis contribute to the degradation.

In order to determine whether thermal or photocatalytic processes govern the sample degradation under SERS condition, potassium iodide (KI) as a photocatalytic scavenger was added, which changes the surface properties of the Ag-SERS substrates and reduces hot carriers, consequently, leading to a suppression of photocatalytic degradation of the sample.<sup>[31]</sup> Clearly, this would not affect thermal degradation. Here, the effect of iodide on sample degradation in SERS studies of dCaL is investigated (see **Figure 2**). Iodide ions are used not only for the previously reported improved reproducibility of SERS spectra (also see Figure S1, Supporting Information),<sup>[32]</sup> but more importantly, to generally suppress sample degradation under mild excitation conditions (Figure 2b) for the first time. The SERS spectra of dCaL were acquired from 10  $\mu\text{L}$  of a 140  $\mu\text{mol L}^{-1}$  dCaL liquid samples mixed with and without 5  $\text{mmol L}^{-1}$  KI, respectively. Simply adding KI to a dCaL solution resulted in a clean SERS spectrum of dCaL. Each spectrum was acquired at a laser power of 1 mW and was

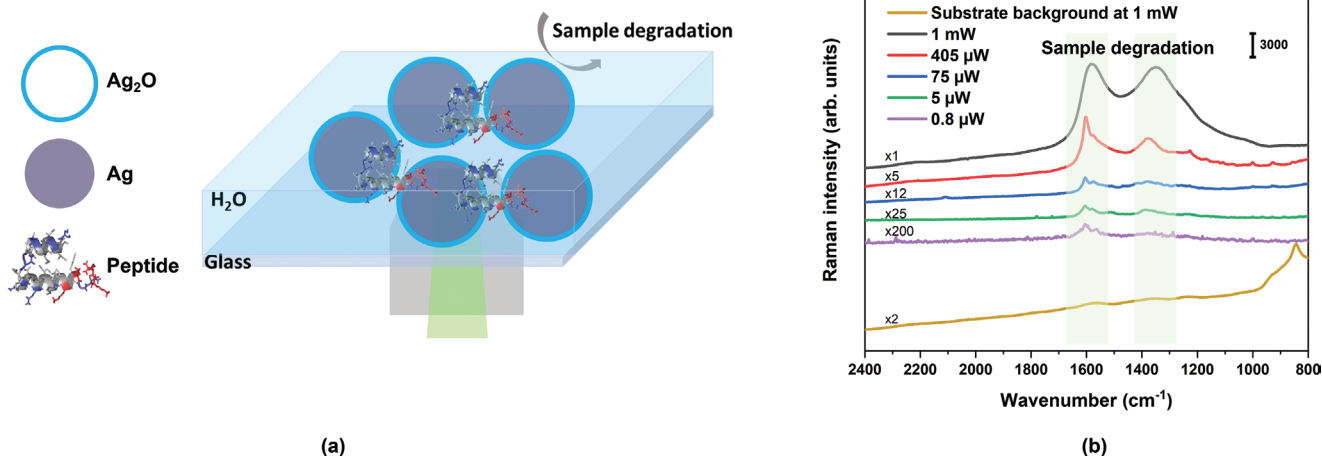


**Figure 1.** a) Sketch of a SERS experiment on a PVD-fabricated Ag substrate in liquid. b) Raman spectra of dCaL on Ag-SERS substrates at 5 different laser powers. Sample degradation can be clearly observed. (The peptide model is provided by the courtesy of Prof. Thomas Gutschmann, FZ Borstel).

averaged from 300 accumulations with 1 s acquisition time. The indicative C–D stretching and ring breathing modes of phenylalanine from dCaL appear at 2290 and 960  $\text{cm}^{-1}$ , respectively. Moreover, the iodide treated SERS spectrum matches the conventional Raman spectrum surprisingly well (Figure 2c), indicating that the iodide does not introduce further signals and that no specific orientation effects due to peptide substrate interaction are detected. The conventional Raman spectrum of 10  $\mu\text{L}$  of a 1.4  $\text{mmol L}^{-1}$  dCaL dry sample was averaged from 10 accumulations with 10 s acquisition time at a laser power of 14.8 mW. In contrast, the SERS spectrum was acquired from 10  $\mu\text{L}$  of a 140  $\mu\text{mol L}^{-1}$  dCaL solution at a laser power of 26  $\mu\text{W}$  with 1 s acquisition time and 300 accumulations. The two spectra adequately match each other, and the characteristic bands (labeled with green columns) are assigned to relative C–D stretching, Amide I band, ring breathing mode, etc. Without iodide, only the signals for a burned sample with the typical two broad bands could be obtained (Figure 2b). Moreover, adding iodide allows to detect dCaL at a concentration down to 1.4  $\mu\text{M}$  and no clear variation, apart from the expected intensity changes, was observed at different dCaLs concentrations which indicates that no potential interaction between dCaL and Ag particles leading to photo-decomposition is present (Figure S2, Supporting Information). In general, a concentration of 5  $\text{mmol L}^{-1}$  iodide was found to efficiently suppress sample degradation and sufficiently improve the signal-to-noise-ratio (SNR); however, the detailed stoichiometric ratio of iodide to samples is still unclear. Previous reports have mentioned that the iodination of Ag will improve the physical properties.<sup>[33,34]</sup> Additionally, we also compared the difference of iodide pre-treated substrates with and without iodide solutions in Figure 2d which will be discussed later. However, the suppression effect of iodide on sample degradation in SERS had, to the best of our knowledge, so far never been reported.

## 2.2. Confirmation of Photocatalytic Effects Suppressed by Iodide Using Surface Property Studies

As a p-type semiconductor,<sup>[35]</sup> holes formed on  $\text{Ag}_2\text{O}$  are the main hot carriers, which will also dominate the oxidative ability

of the whole  $\text{Ag}_2\text{O}@Ag$  heterostructure. Once such a SERS substrate is irradiated, the energy is partially transferred to the  $\text{Ag}_2\text{O}$ , and thus, induces the formation of holes, while non-radiative plasmon decay-induced electrons accumulate in the non-oxidized surface areas of the Ag nanoparticles. Hence, the formed hot carriers are well separated, and therefore exhibit increased lifetimes. In an ESR experiment, a spin trap 5-*tert*-butoxycarbonyl-5-methyl-1-pyrroline-*N*-oxide (BMPO) was used to capture potential radicals. While some BMPO radical was clearly detected, it was not possible to assign this to the known  $\text{BMPO}\cdot\text{OH}$  or  $\text{BMPO}\cdot\text{O}_2$  radicals (Figure S3, Supporting Information). Being beyond the scope of this study, this radical was not further explored. Importantly, a so far unknown radical was formed upon laser irradiation of the SERS substrates which is neither  $\cdot\text{O}_2^-$  nor  $\text{OH}\cdot$  radical, which has to be considered as a potential initiator for unpecific reactions.

As shown out in Figure 2, iodide significantly inhibits sample degradation on Ag-SERS substrates. Based on the previous considerations, there are now two possibilities to suppress photocatalysis of the  $\text{Ag}_2\text{O}@Ag$  while at the same time retaining the plasmonic signal enhancement capabilities of the Ag. One way would be the replacement of the formed  $\text{Ag}_2\text{O}$  with a wider bandgap material, while another is to quickly deplete the formed hot carriers. To identify a suitable mechanism regarding the observed effect of iodide, further investigations of the iodide treated Ag-SERS substrates were performed. In terms of the hypothesis of  $\text{Ag}_2\text{O}$  replacement, at first the corresponding solubility in aqueous media has to be considered. Due to the much lower solubility of AgI in water ( $3 \times 10^{-9}$   $\text{g mL}^{-1}$ , 20 °C) compared to  $\text{Ag}_2\text{O}$  ( $1.3 \times 10^{-5}$   $\text{g mL}^{-1}$ , 20 °C), it is conceivable that iodide ions simply replace the oxygen of the  $\text{Ag}_2\text{O}$  layer resulting in a terminating AgI layer. Consequently, this AgI layer reduces the photocatalytic activity of  $\text{Ag}_2\text{O}@Ag$ . Indeed, X-ray photoelectron spectroscopy (XPS) measurements of the iodide treated Ag-SERS substrates confirmed the presence of iodide on its surface (Figure S4, Supporting Information). Furthermore, X-ray diffraction (XRD) experiments revealed weak signals indicating a hexagonal phase of AgI on the surface (Figure S5, Supporting Information). XPS and XRD results jointly confirmed the existence of

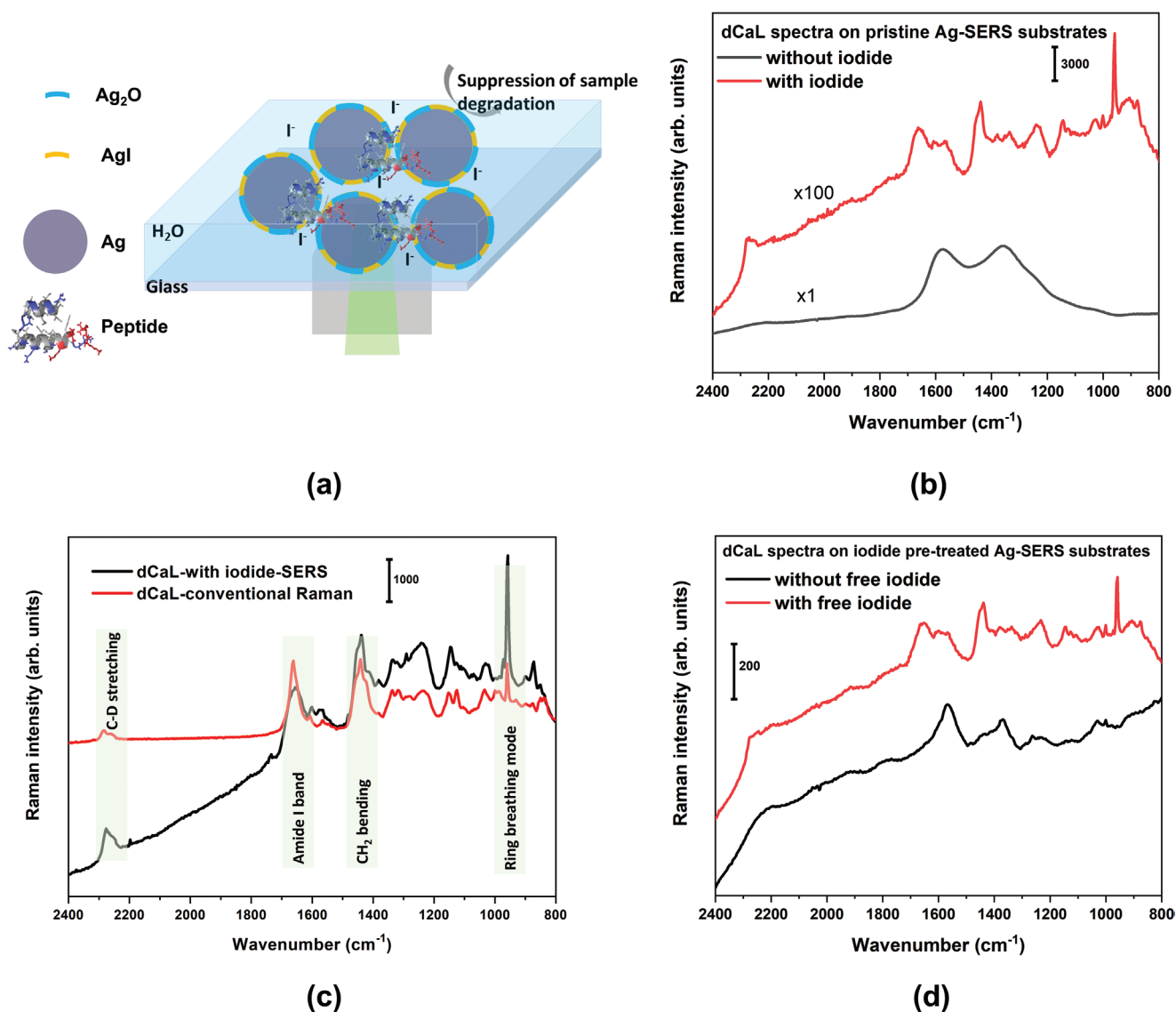


**Figure 2.** a) Sketch of a SERS experiment on a PVD-fabricated Ag substrate in liquid after iodide treatment. b) Comparison of dCaL Raman spectra treated with and without iodide on pristine Ag-SERS substrates. c) Comparison of SERS and conventional (background corrected) Raman spectra of dCaL. d) SERS spectra of dCaL acquired on iodide pre-treated Ag SERS substrates with and without iodide solution. See text for sample preparation details.

trace amount of  $\text{Ag}_2\text{O}$ . Although, these elemental composition changes on the Ag-SERS substrates after iodide treatment corroborate the assumption of a  $\text{Ag}_2\text{O}$  replacement by  $\text{I}^-$  ions, the determination of the underlying mechanisms of the depletion of sample degradation requires further investigations of the electrical properties.

In addition to these classical approaches for accessing photocatalytic processes, Kelvin probe force microscopy (KPFM) was applied for a comparative study of the surface potential of pristine and iodide treated Ag-SERS substrates. This enables the exploration of the local electron density of these substrates under different illumination conditions. Here, KPFM investigations of Ag-SERS substrates under dark and illuminated conditions were carried out, in order to investigate possible light-induced surface potential changes. KPFM is ideally suited

to probe potential photocatalytic effects associated to  $\text{Ag}_2\text{O}@Ag$  and  $\text{AgI}@Ag$  heterostructures. **Figure 3a** manifests that the pristine Ag-SERS substrate has a relatively positive charge under dark conditions, which apparently decreased once the laser was switched on. This phenomenon indicates charge separation process on the substrate. Consequently, KPFM enables the detection of an apparent photocatalytic process originating from the substrate under illumination. Subsequently, the pristine substrate was treated with  $1 \text{ mmol L}^{-1}$  KI for 30 min. No obvious topography changes of the substrate before and after irradiation were detected. The KPFM investigations of the iodide treated Ag-SERS substrate, however, clearly reveal a lower surface potential compared to the pristine substrate due to the high affinity of iodide to Ag.<sup>[31]</sup> As AgI has a bandgap of  $\approx 2.6 \text{ eV}$  (compared to  $\text{Ag}_2\text{O}$ ,  $\approx 1.2 \text{ eV}$ ) which cannot be excited by the 532 nm laser,<sup>[36]</sup> it is

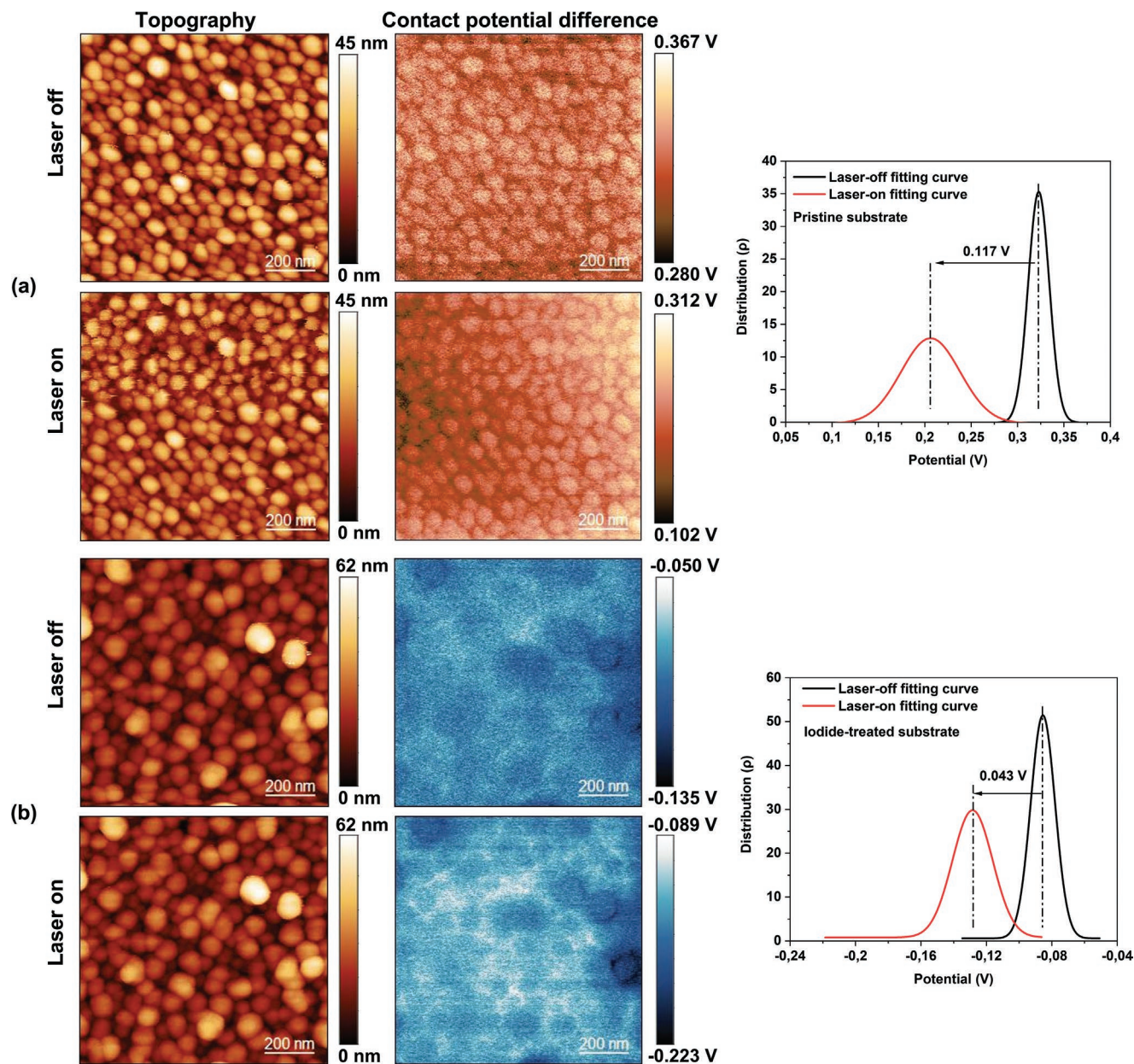


**Figure 3.** The surface potential maps (middle column) and topographies (left column) of a) pristine Ag-SERS and b) iodide-treated Ag-SERS substrates measured by Kelvin probe force microscopy. In the right column the respective averaged potential curves for the two substrates are shown.

expected that the photocatalytic effect of the pristine substrate will be reduced after iodide treatment. Additionally, as iodide is an n-type dopant, the Fermi level of AgI will be shifted to a higher value compared to the one of  $\text{Ag}_2\text{O}$ .<sup>[31]</sup> This will further affect the charge separation of the AgI@Ag structure referred to the original  $\text{Ag}_2\text{O}$ @Ag structure. Figure 3b shows a further decrease of the surface potential (from 0.367 to  $-0.135$  V) on the substrate under illumination indicating the occurrence of charge separation and verifies our hypothesis. Furthermore, the smaller light-induced surface potential shift of the AgI@Ag system (0.043 V) compared to the potential change of the pristine substrate (0.117 V) indicates less generation of hot carriers in the AgI@Ag system and consequently reduced potential photocatalytic activity. This explains the observation in Figure 2d where the

iodide pre-treated substrate shows diminished yet present degradation. It is likely that this remaining degradation originates from the residual plasmon decay-induced hot carriers but it is also possible from the residual  $\text{Ag}_2\text{O}$ . At the same time, this also indicates that free iodide plays a role in the observed suppression of sample degradation.

### 2.3. Resolving the Effects of Iodide on the Suppression of Sample Degradation in Ag-SERS

To understand the effect of iodide in Ag-SERS substrate investigations, the difference of iodide coating of the Ag-SERS substrates versus addition of iodide to the sample solutions is

further investigated, to differentiate the effects of iodide as a surface compound and as a solute. Figure 2d presents a SERS spectrum of dCaL recorded on an iodide pre-treated Ag SERS substrate and compares it to a spectrum recorded using an iodide pre-treated substrate with and without free iodide in the solution. The substrate was immersed in a 5 mmol L<sup>-1</sup> KI solution for 30 min and then rinsed with dH<sub>2</sub>O for the following measurements. 2 μL of 140 μmol L<sup>-1</sup> dCaL were firstly measured on the substrate and then 0.5 μL of a 50 mmol L<sup>-1</sup> KI solution was added to the sample. The spectra were acquired using 1 mW laser power and were averaged from 100 accumulations of 1 s acquisition time, respectively. Without excess solute iodide in the dCaL sample, the quality of the Raman spectrum of dCaL is still seriously affected by sample degradation, similar to measurements on untreated SERS substrates. A clean dCaL SERS spectrum was only obtained once excess iodide was applied. In agreement with above KPFM considerations, this leads to the assumption that the direct replacement of Ag<sub>2</sub>O to AgI does contribute only slightly to the suppression of sample degradation at 532 nm excitation. Consequently, free iodide ions in the solution must affect the suppression process. This result suggests that the sample degradation is most effectively prevented by an instantaneous depletion of the formed hot carriers in the Ag<sub>2</sub>O@Ag and AgI@Ag systems, i.e., the freely diffusing I<sup>-</sup> ions in the solution act as scavengers for the hot holes.

Interestingly, other halogen ions (Cl<sup>-</sup> and Br<sup>-</sup>) do not suppress the sample degradation (Figure S6, Supporting Information). Thus, electrostatic interaction only cannot be the main reason for degradation suppression by iodide, but likely improves the signal enhancement capabilities through a tight analyte–substrate interaction. Additionally, Cl<sup>-</sup> and Br<sup>-</sup> are also able to react with Ag<sub>2</sub>O converting it into AgCl (solubility in water, 1.6 × 10<sup>-6</sup> g mL<sup>-1</sup>, 20 °C) and AgBr (solubility in water, 1.4 × 10<sup>-7</sup> g mL<sup>-1</sup>, 20 °C) respectively. However, sample degradation is still observed in the presence of these ions which is in agreement with the iodide case above. Consequently, we will mainly discuss the effects induced by iodide in the further discussion and focus next on the involved redox potentials.

Reactions induced by Ag<sub>2</sub>O@Ag in an iodide environment can also be explained considering the redox potential of each reactant. It has been reported that the conduction band of Ag<sub>2</sub>O is around +0.3 V (vs NHE, pH 7), which is not sufficient to reduce O<sub>2</sub> to ·O<sub>2</sub><sup>-</sup> (-0.046 V, vs NHE, pH 7) radicals.<sup>[37]</sup> However, these electrons may possibly reduce O<sub>2</sub> to H<sub>2</sub>O<sub>2</sub> (2e<sup>-</sup> + 2H<sup>+</sup> + O<sub>2</sub> → H<sub>2</sub>O<sub>2</sub>, +0.27 V, vs NHE, pH 7) or H<sub>2</sub>O (4e<sup>-</sup> + 4H<sup>+</sup> + O<sub>2</sub> → 2H<sub>2</sub>O, +0.82 V, vs NHE, pH 7) by multielectron-transfer routes.<sup>[35]</sup> Accordingly, the valence band of Ag<sub>2</sub>O is at around +1.5 V which is insufficient to oxidize H<sub>2</sub>O into OH· radicals (≈+2.3 V, vs NHE, pH 7).<sup>[38]</sup> This well supports the above-mentioned ESR experiment, where neither BMPO·OH nor BMPO·O<sub>2</sub>· radicals were detected. In comparison, the redox potentials of I<sub>3</sub><sup>-</sup>/I<sup>-</sup> and IO<sub>3</sub><sup>-</sup>/I<sup>-</sup> are around +0.55 V and +1.09 V (vs NHE, pH 7),<sup>[39,40]</sup> respectively, which could be easily oxidized by the valence band of Ag<sub>2</sub>O (Figure 4a), i.e., the holes will be quickly depleted by free iodide. This process could be expressed in the following reaction equations:



or alternatively,



Moreover, the valence band of AgI is at around 2.13 V.<sup>[41]</sup> In contrast, the redox potentials of Cl·/Cl<sup>-</sup> and Br·/Br<sup>-</sup> are around +2.43 V and +1.96 V,<sup>[38]</sup> respectively, which explains why these anions, contrary to iodide, do not suppress dCaL degradation. Even though the redox reactions of amino acids in SERS are not well studied yet, it has been mentioned that amino acids and peptides are easily oxidized.<sup>[42]</sup> If iodide can protect the peptide dCaL from photocatalysis-induced degradation, it means iodide has a relatively lower oxidative potential than the peptide which inhibits the oxidation of amino acids and/or the peptide. Therefore, it is proposed that the redox potential of I<sub>3</sub><sup>-</sup>/I<sup>-</sup> or IO<sub>3</sub><sup>-</sup>/I<sup>-</sup> is much lower than those of amino acids/proteins in dCaL (often around or larger than 1 V)<sup>[43–45]</sup> and further protects the peptides. Furthermore, according to the redox potential of IO<sub>3</sub><sup>-</sup>/I<sup>-</sup>, electrons cannot reduce IO<sub>3</sub><sup>-</sup> into I<sup>-</sup>. In the Figure S7 (Supporting Information), Ag-SERS investigations utilizing KIO<sub>3</sub> instead of KI also verified that iodate has a limited effect and cannot prevent sample degradation, which indirectly indicates that hot electrons barely impact the degradation process of this peptide in contrast to the hot holes. Finally, we propose that free iodide dominates in the suppression of sample degradation with its lower redox potential compared to peptides.

Based on these results, a mechanism of sample degradation and suppression on Ag-SERS substrates is proposed in Figure 4b. The plasmonic Ag-SERS substrate is represented by a single AgNP, which is partially or fully covered by Ag<sub>2</sub>O, thus forming an Ag<sub>2</sub>O@Ag heterostructure. This heterostructure can act as a plasmon-assisted photocatalyst. Once irradiated by light with an energy matching the plasmon resonance, electron/hole pairs are induced by plasmon decay and a charge separation/transfer occurs between Ag<sub>2</sub>O and Ag leading to an increased lifetime of these hot carriers. Ag<sub>2</sub>O acts as a pool for holes while Ag becomes a reservoir for the electrons. The extended lifetime of the hot carriers and matching energy levels between peptide and the carries are the main reason for sample degradation. Once iodide solution is injected, iodide will react with Ag<sub>2</sub>O. The formed AgI has a much broader bandgap which cannot be excited by a 532 nm laser. Even though the coupling effect between AgI and Ag nanoparticles is unclear here, the weaker charge separation of AgI@Ag compared to the Ag<sub>2</sub>O@Ag structure, detected by KPFM, directly relates to a reduced photocatalytic effect. Considering that hot carriers from plasmon decay of Ag nanoparticles could also induce apparent photocatalytic reactions, the diminished sample degradation on the iodide-modified Ag substrate in Figure 2d fits this conclusion. Notably, the interaction of iodide and Ag<sub>2</sub>O/Ag substrates is difficult to assess quantitatively as it is highly affected by experimental conditions, e.g., the substrate quality and the specific reaction kinetics of iodide on such a substrate. Furthermore, a systematic, i.e., quantitative evaluation of the AgI/Ag heterojunction would be also desirable from a general point of view. It is expected these issues will be addressed in the future at this stage, the qualitative aspects of photo-damage suppression can be addressed without such detailed information.

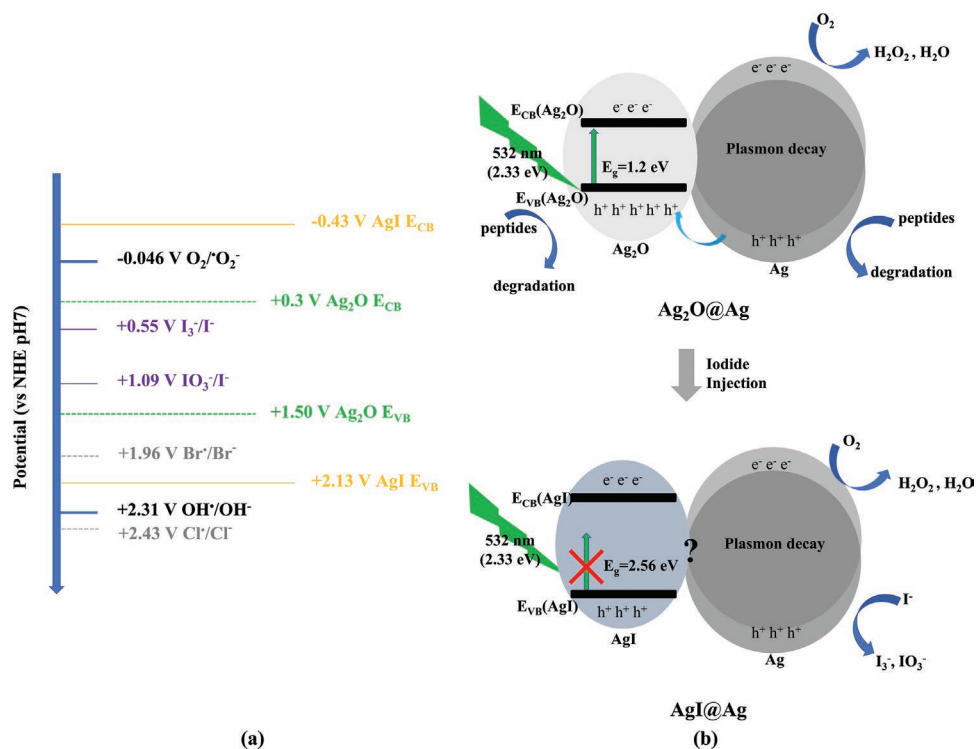


**Figure 4.** a) Involved redox potentials versus NHE at pH 7. The conduction band and valence band of  $\text{Ag}_2\text{O}$  are at +0.3 V and +1.5 V (green), the respective potentials of AgI (−0.43 and +2.13 V) are shown in yellow. The other potential redox pairs are also added for comparison. b) Proposed sketch of the mechanism of iodide induced degradation suppression, nicely demonstrating the effect of iodide induced hole depletion that protects the peptides from oxidation.

Consequently, this study reveals that iodide suppresses sample degradation in Ag-SERS measurements not only by the replacement of  $\text{Ag}_2\text{O}$  into AgI but more importantly by the depletion of hot carriers from the whole structure. Last but not least, the discussed iodide method shows a selectivity toward peptides as shown by a comparison of Melittin and p7a as examples for positively and negatively charged peptides, respectively (Figure S8, Supporting Information). It seems that the iodide method performs better on positively charged peptides, most likely due to favorable electrostatic interactions. Based on our results, we propose that any hot-carrier scavenger with a suitable redox potential matching the redox relation between hot carriers and sample should be able to suppress sample degradation induced by photocatalysis.

### 3. Conclusion

In summary, this study demonstrates for the first time that free solute iodide enables the suppression of peptide degradation on Ag-SERS substrates (PVD method) in liquid environment, and thus, goes beyond the previously observed effect of improving reproducibility of SERS spectra. It is proposed that, besides the commonly suggested thermal effect, plasmon-assisted photocatalysis of  $\text{Ag}_2\text{O}@Ag$  plays a critical role in sample degradation on pristine (PVD) Ag-SERS substrates. Firstly, the role of free iodide was unveiled by measurements on iodide pre-treated substrates with and without iodide solution. More importantly,

Kelvin probe force microscopy directly verifies the existence of photocatalytic activity on such Ag-SERS substrates by revealing the decrease of surface potential once the substrate was irradiated indicating the occurrence of a photocatalytic charge separation process. Additionally, detailed investigations on the chemical and physical surface properties combined with considerations of the known redox potential of the involved species further allowed proposing a mechanism for the protective effect of iodide, i.e., hot holes induced from  $\text{Ag}_2\text{O}@Ag$  are efficiently depleted by iodide ions, which suppress peptide degradation. Even though the exact mechanism is not fully clear yet, the effects of iodide in Ag-SERS measurements are obvious. Consequently, this study paves the way toward biological related SERS investigations under physiological conditions, which are currently hampered by sample degradation.

### 4. Experimental Section

**Materials:** Candidalysin (CaL) is a cytolytic peptide secreted by the opportunistic fungal pathogen *Candida albicans* (please see the model of CaL in Figure S9, Supporting Information).<sup>[46]</sup> The phenylalanine-deuterated form (d5-Phe) of CaL (dCaL, sequence: SIIGIIMGILGNIPQVIQIIMSIVKAFKGNK, from PeptideSynthetics, UK) is used as a model sample in this work. KI, KBr, KCl and  $\text{KIO}_3$  (SigmaAldrich, USA) solutions were used as a source of iodide, bromide, chloride and iodate ions. Melittin (sequence: GIGAVLKVLTTGLPALISWIKRKRQQ, from Proteogenix, France) and p7a (sequence: DGLDFLDELLQRLPQLIT, from PeptideSynthetics, UK) are used as positively and negatively charged control peptides. All peptide

samples were dissolved into deionized water and had pH values around 6 to 7.

**Characterization:** The preparation of Ag-SERS substrates followed the previously reported procedure.<sup>[47]</sup> Their reproducibility with respect to enhancement and spectral variation has been evaluated previously.<sup>[48]</sup> Deviating from this procedure, coverslips coated with a 3 nm chromium layer were used, which increases the stability of the Ag-SERS substrates in liquid environments and also the conductivity of substrates. Kelvin probe force microscopy was used to measure the surface potentials of these substrates using a JPK NanoWizard ULTRA Speed system (Bruker Nano, Germany), which also acquires the topographies of Ag-SERS substrates before and after iodide treatment at the same time. ESR (Elexsys E580, Bruker, BioSpin) was used to investigate the presence of radicals. XPS measurements were performed in an ultra-high vacuum (UHV) Multiprobe System (Scienta Omicron) with a base pressure of  $2 \times 10^{-10}$  mbar. A monochromatic Al K $\alpha$  X-ray source was used in combination with an electron energy analyzer (Argus CU) employing a spectral energy resolution of 0.6 eV and a photoelectron emission angle with respect to the surface normal of 19° and XRD (X'pert Pro MPD, Malvern Panalytical, Netherlands) were used to analyze the elements and crystal phases on the substrates, respectively. Detailed information regarding the substrate analysis is provided in the Supporting Information.

**Raman-Related Experiments:** For all Raman experiments a 532 nm laser was used as light source. This wavelength matches the plasmon resonance of the silver island substrates (see Figure S10, Supporting Information). An inverted microscope with a  $60 \times 1.45$  N.A. objective (Olympus, Japan) was used as working stage. Powers, acquisition time, and number of accumulations are specified for each experiment, respectively. Different concentrations of dCaL were used in conventional Raman and SERS experiments which are specified when used. All SERS spectra were acquired from liquid samples which were dropped onto SERS substrates and were measured immediately without any drying steps. The C–D stretching and ring breathing mode of dCaL are found at 2290 and 960 cm<sup>-1</sup>, respectively and used as marker bands to verify adsorption. The Si signal at 519 cm<sup>-1</sup> was used as calibration. No background subtraction was applied to all SERS spectra.

## Supporting Information

Supporting Information is available from the Wiley Online Library or from the author.

## Acknowledgements

The authors acknowledge the financial support from the Leibniz Science Campus InfectoOptics SAS-2015-HKI-LWC. Discussions with Prof. Caijin Huang, Dr. Zuyang Zheng, and Dr. Zhibin Fang regarding photocatalysts and photocatalysis are highly acknowledged. V.D. and A.T. acknowledge support from the German Science Foundation via the CRC 1375 “NOA” project B2 and C2. W.P. acknowledges support by the German Research Foundation (DFG) through grant No. INST 275/406-1 FUGG. C.H. and S.H. acknowledge support from Collaborative Research Center PolyTarget 1278, B4. and C4 (project No. 316213987).

Open access funding enabled and organized by Projekt DEAL.

## Conflict of Interest

The authors declare no conflict of interest.

## Data Availability Statement

The data that support the findings of this study are available from the corresponding author upon reasonable request.

## Keywords

Ag-surface-enhanced Raman spectroscopy (SERS), hot carriers, iodides, Kelvin probe force microscopy, peptides, sample degradation

Received: August 18, 2022

Revised: October 10, 2022

Published online: November 7, 2022

- [1] K. J. I. Ember, M. A. Hoeve, S. L. McAughtrie, M. S. Bergholt, B. J. Dwyer, M. M. Stevens, K. Faulds, S. J. Forbes, C. J. Campbell, *NPJ Regener. Med.* **2017**, 2, 12.
- [2] J. Langer, D. J. de Aberasturi, J. A. Aizpurua, R. A. Alvarez-Puebla, B. Auguie, J. J. Baumberg, G. C. Bazan, S. E. J. Bell, A. Boisen, A. G. Brolo, J. Choo, D. Cialla-May, V. Deckert, L. Fabris, K. Faulds, F. J. G. de Abajo, R. Goodacre, D. Graham, A. J. Haes, C. L. Haynes, C. Huck, T. Itoh, M. Käll, J. Kneipp, N. A. Kotov, H. Kuang, E. C. Le Ru, H. K. Lee, J.-F. Li, X. Y. Ling, et al., *ACS Nano* **2020**, 14, 28.
- [3] E. C. Le Ru, E. Blackie, M. Meyer, P. G. Etchegoin, *J. Phys. Chem. C* **2007**, 111, 13794.
- [4] C. Zong, M. Xu, L.-J. Xu, T. Wei, X. Ma, X.-S. Zheng, R. Hu, B. Ren, *Chem. Rev.* **2018**, 118, 4946.
- [5] A. B. Zrimsek, N. Chiang, M. Mattei, S. Zaleski, M. O. McAnally, C. T. Chapman, A. I. Henry, G. C. Schatz, R. P. Van Duyne, *Chem. Rev.* **2017**, 117, 7583.
- [6] K. F. Domke, D. Zhang, B. Pettinger, *J. Phys. Chem. C* **2007**, 111, 8611.
- [7] A. Kudelski, B. Pettinger, *Chem. Phys. Lett.* **2000**, 321, 356.
- [8] C. Heck, Y. Kanehira, J. Kneipp, I. Bald, *Molecules* **2019**, 24, 2324.
- [9] C. Blum, T. Schmid, L. Opilik, S. Weidmann, S. R. Fagerer, R. Zenobi, *J. Raman Spectrosc.* **2012**, 43, 1895.
- [10] M. Veres, M. Füle, S. Tóth, M. Koós, I. Pócsik, *Diamond Relat. Mater.* **2004**, 13, 1412.
- [11] A. Gellé, T. Jin, L. de la Garza, G. D. Price, L. V. Besteiro, A. Moores, *Chem. Rev.* **2020**, 120, 986.
- [12] A. O. Govorov, H. H. Richardson, *Nano Today* **2007**, 2, 30.
- [13] J. B. Herzog, M. W. Knight, D. Natelson, *Nano Lett.* **2014**, 14, 499.
- [14] Z.-C. Zeng, H. Wang, P. Johns, G. V. Hartland, Z. D. Schultz, *J. Phys. Chem. C* **2017**, 121, 11623.
- [15] D. J. Sharkey, E. R. Scalice, K. G. Christy, Jr., S. M. Atwood, J. L. Daiss, *Nat. Biotechnol.* **1994**, 12, 506.
- [16] M. Richard-Lacroix, V. Deckert, *Light: Sci. Appl.* **2020**, 9, 35.
- [17] K. Chen, H. Wang, *Mol. Syst. Des. Eng.* **2021**, 6, 250.
- [18] X. Zhang, Y. L. Chen, R.-S. Liu, D. P. Tsai, *Rep. Prog. Phys.* **2013**, 76, 046401.
- [19] H. Reddy, K. Wang, Z. Kudyshev, L. Zhu, S. Yan, A. Vezzoli, S. J. Higgins, V. Gavini, A. Boltasseva, P. Reddy, V. M. Shalaev, E. Meyhofer, *Science* **2020**, 369, 423.
- [20] J. Schneider, M. Matsuoka, M. Takeuchi, J. Zhang, Y. Horiuchi, M. Anpo, D. W. Bahnemann, *Chem. Rev.* **2014**, 114, 9919.
- [21] R. Sundararaman, P. Narang, A. S. Jermyn, W. A. Goddard, III, H. A. Atwater, *Nat. Commun.* **2014**, 5, 5788.
- [22] Y. Han, R. Lupitsky, T.-M. Chou, C. M. Stafford, H. Du, S. Sukhishvili, *Anal. Chem.* **2011**, 83, 5873.
- [23] N. Michieli, R. Pilot, V. Russo, C. Scian, F. Todescato, R. Signorini, S. Agnoli, T. Cesca, R. Boziob, G. Mattei, *RSC Adv.* **2017**, 7, 369.
- [24] Y. Xu, M. A. A. Schoonen, *Am. Mineral.* **2000**, 85, 543.
- [25] H. Xu, J. Xie, W. Jia, G. Wu, Y. Cao, *J. Colloid Interface Sci.* **2018**, 516, 511.
- [26] X. Wang, S. Li, H. Yu, J. Yu, S. Liu, *Chemistry* **2011**, 17, 7777.
- [27] G. Wang, X. Ma, B. Huang, H. Cheng, Z. Wang, J. Zhan, X. Qin, X. Zhang, Y. Dai, *J. Mater. Chem.* **2012**, 22, 21189.
- [28] R. Geßner, P. Rösch, R. Petry, M. Schmitt, M. A. Strehle, W. Kiefer, J. Popp, *Analyst* **2004**, 129, 1193.



- [29] S. Bernardini, F. Bellatreccia, G. D. Ventura, P. Ballirano, A. Sodo, *RSC Adv.* **2020**, *10*, 923.
- [30] P. K. Jain, *J. Phys. Chem. C* **2019**, *123*, 24347.
- [31] A. Stefancu, S. Lee, L. Zhu, M. Liu, R. C. Lucacel, E. Cortés, N. Leopold, *Nano Lett.* **2021**, *21*, 6592.
- [32] L.-J. Xu, C. Zong, X.-S. Zheng, P. Hu, J.-M. Feng, B. Ren, *Anal. Chem.* **2014**, *86*, 2238.
- [33] C. Yang, Y.-T. Xie, M. M.-F. Yuen, B. Xu, B. Gao, X. Xiong, C. P. Wong, *Adv. Funct. Mater.* **2010**, *20*, 2580.
- [34] M. Y. Bashouti, R. Talebi, T. Kassar, A. Nahal, J. Ristein, T. Unruh, S. H. Christiansen, *Sci. Rep.* **2016**, *6*, 21439.
- [35] J. Wei, Y. Lei, H. Jia, J. Cheng, H. Hou, Z. Zheng, *Dalton Trans.* **2014**, *43*, 11333.
- [36] D. H. Cui, X. C. Song, Y. F. Zheng, *RSC Adv.* **2016**, *6*, 71983.
- [37] S. Akel, R. Dillert, N. O. Balayeva, R. Boughaled, J. Koch, M. El Azzouzi, D. W. Bahnemann, *Catalysts* **2018**, *8*, 647.
- [38] D. A. Armstrong, R. E. Huie, W. H. Koppenol, S. V. Lymar, G. Merényi, P. Neta, B. Ruscic, D. M. Stanbury, S. Steenken, P. Wardman, *Biolnorg. React. Mech.* **2013**, *9*, 1139.
- [39] M. Tabata, K. Maeda, M. Higashi, D. Lu, T. Takata, R. Abe, K. Domen, *Langmuir* **2010**, *26*, 9161.
- [40] Y. Miseki, S. Fujiyoshi, T. Gunji, K. Sayama, *Catal. Sci. Technol.* **2013**, *3*, 1750.
- [41] L. Zhang, A. Zhang, H. Lu, Z. Sun, W. Sheng, L. Sun, J. Xiang, *RSC Adv.* **2017**, *7*, 31448.
- [42] E. R. Stadtman, *Annu. Rev. Biochem.* **1993**, *62*, 797.
- [43] D. M. Close, P. Wardman, *J. Phys. Chem. A* **2018**, *122*, 439.
- [44] M. L. Villegas, S. G. Bertolotti, C. M. Previtali, M. V. Encinas, *Photochem. Photobiol.* **2005**, *81*, 884.
- [45] J. F. O'Donnell, C. K. Mann, *J. Electroanal. Chem. Interfacial Electrochem.* **1967**, *13*, 157.
- [46] D. L. Moyes, D. Wilson, J. P. Richardson, S. Mogavero, S. X. Tang, J. Wernecke, S. Höfs, R. L. Gratacap, J. Robbins, M. Runglall, C. Murciano, M. Blagojevic, S. Thavaraj, T. M. Förster, B. Hebecker, L. Kasper, G. Vizcay, S. I. Iancu, N. Kichik, A. Häder, O. Kurzai, T. Luo, T. Krüger, O. Kniemeyer, E. Cota, O. Bader, R. T. Wheeler, T. Gutschmann, B. Hube, J. R. Naglik, *Nature* **2016**, *532*, 64.
- [47] R. M. Stöckle, V. Deckert, C. Fokas, R. Zenobi, *Appl. Spectrosc.* **2000**, *54*, 1577.
- [48] P. Singh, T. Deckert-Gaudig, H. Schneidewind, K. Kirsch, E. M. van S. Lantman, B. M. Weckhuysen, V. Deckert, *Phys. Chem. Chem. Phys.* **2015**, *17*, 2991.